Uranium Immobilization by Sulfate-Reducing Biofilms Grown on Hematite, Dolomite, And Calcite

ENRICO MARSILI,[†] HALUK BEYENAL,[†,‡] LUCA DI PALMA,[§] CARLO MERLI,[§] ALICE DOHNALKOVA,[||] JAMES, E. AMONETTE,[||] AND ZBIGNIEW LEWANDOWSKI*[,†,⊥]

Center for Biofilm Engineering; Department of Civil Engineering, Montana State University, Bozeman, Montana 59717, School of Chemical Engineering and Bioengineering, Washington State University, Pullman, Washington 99164, Department of Chemical Engineering, University "La Sapienza", Via Eudossiana, 18 00184 Rome, Italy, and Fundamental Sciences Directorate, Pacific Northwest National Laboratory, 790 sixth St., Richland, Washington 99352

Received June 05, 2007. Revised manuscript received September 10, 2007. Accepted September 21, 2007.

Biofilms of sulfate-reducing bacteria *Desulfovibrio desulfuricans* G20 were used to reduce dissolved U(VI) and subsequently immobilize U(IV) in the presence of uranium-complexing carbonates. The biofilms were grown in three identically operated fixed bed reactors, filled with three types of minerals: one noncarbonate-bearing mineral (hematite) and two carbonate-bearing minerals (calcite and dolomite). The source of carbonates in the reactors filled with calcite and dolomite were the minerals, while in the reactor filled with hematite it was a 10 mM carbonate buffer, pH 7.2, which we added to the growth medium. Our five-month study demonstrated that the sulfate-reducing biofilms grown in all reactors were able to immobilize/reduce uranium efficiently, despite the presence of uranium-complexing carbonates.

Introduction

Uranium (U^{238}) has been discharged into the environment for more than 60 years as a result of nuclear energy and weapons production and incorrect mine management. The EPA remediation program lists 21 sites in the U.S. in which uranium contaminates groundwater and soil (*1*). Uranium-contaminated sites pose challenging problems for remediation. One of the promising remediation processes is the in situ microbial reduction of uranium in the subsurface environment, leading to the immobilization of the reduced uranium. Both nonbiological and biological reactions can contribute to the microbially stimulated reduction of uranium.

Nonbiologically, uranium can be reduced by the sulfides or by sulfate-reducing bacteria (*2*, *3*). This process is efficient but it has limited application in natural waters. Even though hydrated uranium (VI) ions in pure water are amenable to reduction by microbially generated hydrogen sulfide, uranium (VI) in natural waters forms complexes with carbonates, and the complexed uranium ions are not amenable to reduction by hydrogen sulfide (*4–6*). Because most natural waters are buffered by the carbonate system and carbonates in groundwaters can reach considerable concentrations (5–20 mM), the feasibility of uranium reduction in the subsoil formation by microbially generated hydrogen sulfide is questionable. When the contaminated water contains carbonates, most of the U(VI) forms complexes, and the chemical reduction of uranium caused by biogenically produced sulfide is not likely to occur (*4*).

Biologically, uranium U(VI) is reduced by the electrons derived directly from organics, and uranium deposits are associated with the microbial membranes. The process is known as enzymatic reduction of uranium, and it can be carried by various microorganizms, not only sulfate reducing bacteria (*7–10*). The exact mechanism of this process is not known but the involvement of c-type cytochromes has been implicated by some authors (*11, 12*). The efficiency of the enzymatic reduction of uranium does not seem to decrease in the presence of uranium complexed with carbonates, which, hypothetically, makes possible uranium removal from contaminated waters using enzymatic reduction. Since the nonbiological reduction has limited application, the enzymatic reduction has been extensively studied. As a result of these studies, Fredrickson et al., 2002; Lovley et al., 1991; Ganesh et al., 1999; and Fredrickson et al., 2000, among others, have shown that U(VI) can be reduced to U(IV) by several bacterial strains, such as *Desulfovibrio desulfuricans*, *Shewanella putrefaciens*, and *Deinococcus radiodurans* which use U(VI) as an electron acceptor (*13–16*). However, it is not clear whether the enzymatic reduction of uranium is efficient enough to remove considerable concentrations of uranium in the contaminated groundwaters and whether the possible toxic effects of uranium to microorganisms make the process sustainable for long periods of time.

Our study has been designed to test the hypothesis that uranium U(VI) can be reduced in the subsoil formation by biofilms of sulfate-reducing bacteria (SRB) in the presence of carbonates and that the process is efficient and sustainable for long time. To test this hypothesis, we used SRB biofilms of *Desulfovibrio desulfuricans* G20 grown in three fixed bed tubular reactors, each filled with hematite, calcite, or dolomite, and we used lactate as the electron donor. The growth medium supplied to the reactors filled with calcite and dolomite was not buffered, since we expected that carbonates from the carbonate-bearing minerals would buffer the solution. The growth medium supplied to the reactor filled with hematite was buffered with 10 mM carbonate. Uranium U(VI) was continuously supplied to all reactors and the removal rate was evaluated from the mass balances in the influents and effluents of the reactors. After five months of operation, Biofilm samples were taken from the reactors and were analyzed using high-resolution transmission electron microscopy (HRTEM), energy-dispersive X-ray spectroscopy (EDS), X-ray photoelectron spectroscopy (XPS), and selected-area electron diffraction (SAED) to determine the chemistry and crystallography of the uranium deposits.

Materials and Methods

Microorganizm and Growth Medium. *D. desulfuricans* G20, obtained by courtesy of J. Wall, University of Missouri, Columbia, was subcultured and maintained in a modified metal toxicity medium amended with reductants (ascorbic acid and sodium thyoglycolate), as described by Sani et al.,

* Corresponding author phone: 1-406-994-5915; fax: 1-406-994-6098; e-mail: ZL@erc.montana.edu.
[†] Center for Biofilm Engineering, Montana State University.
[‡] Washington State University.
[§] University "La Sapienza".
[||] Pacific Northwest National Laboratory.
[⊥] Department of Civil Engineering, Montana State University.

10.1021/es071335k CCC: $37.00
Published on Web 11/08/2007

2001 (*17*). The growth media, described in Table S1 in the Supporting Information (SI), were prepared using deionized water and were autoclaved at 121 ± 1 °C (1 atm vapor pressure) for 20 min The details of growth media are described in Table S1, SI. Briefly, three types of growth media were used: medium A was used to grow the stock culture of the microorganizms, B1 to grow biofilms in the reactors filled with dolomite and calcite, and C2 to grow biofilms in the reactor filled with hematite. Filter-sterilized (0.2 μm filter) uranyl acetate (Mallinckrodt, MO) was added, to growth media B2 and C2 only, to a final U(VI) concentration of 126 μM. A three step procedure was used: (1) grow the microorganisms and inoculate the reactors, (2) operate the reactors to establish the presence of the biofilms in the absence of uranium, and (3) operate the reactors in the presence of uranium. The procedures for inoculating and operating the reactors are described later.

Packing Material. Hematite, calcite, and dolomite were used as the packing materials. Synthetic polycrystalline hematite beads, 4 × 4 mm in cross section and 4, 8, or 13 mm in length, were obtained from a jewelry supplier (Harlequin Beads and Jewelry, Eugene, OR). Analysis by X-ray diffraction showed them to be hematite with traces (ca. 1 wt%) of magnetite. The identical diffraction patterns obtained for powdered beads and intact beads confirmed their polycrystalline nature. The bead surfaces were cleaned by rinsing with a series of organic solvents (in the order hexane, acetone, methanol, and 2-propanol) followed by a 60 min exposure to ozone using an ozone plasma generator. Cleaned beads were then wrapped in Al foil until use. XPS analysis showed the cleaned bead surfaces to deviate from the nominal bulk composition of hematite by having more oxygen, less iron, and minor amounts of C, Al, and Si impurities (Table S2, SI). After sputtering to remove the top 20 nm of the surface, XPS analysis showed a composition closer to the nominal bulk hematite composition.

Commercial dolomite from the Regal Talc Mine (Dillon, MT) was bought from a local construction material supplier, and hexagonal calcite was obtained from Sargent-Welch, Science and Education Supply. The minerals were crushed with a hammer and sieved. The size fraction in the range 3.35–4.76 mm was used as the packing material, and the minerals were rinsed with deionized water before they were used. The commercial dolomite, $CaMg(CO_3)_2$, contained small amounts of iron. This was determined by visual inspection, which showed spots of hematite filling the cracks of the dolomite, and confirmed by the presence of a Fe peak in the EDS analysis (results not shown).

Column Reactors. The reactors were clear polycarbonate tubes (internal diameter 2.54 cm, length 40 cm) (Figure S1, SI). Each column was filled with 132 mL of crushed mineral and then sealed with epoxy resin to prevent air access. The pore volume in each of the reactors was 70 mL. To ensure the uniform delivery of growth media, we used flow distributors made of 0.5 cm glass beads entrapped between two plastic sieves; these were placed in the inlet and in the outlet of the column reactors (Figure S1, SI). A mixing chamber (0.5 L of volume) was located in the recycle line, as shown in Figure S1, SI. The procedures of growing the biofilms and operating the reactors are described in the Supporting Information.

Carbonates and Other Major Species in the Effluents. The concentrations of soluble carbonates and other major species at equilibrium with the packing material were calculated for each biofilm reactor, using the software Visual MINTEQ version 2.51 (KTH, Stockholm, Sweden). For the computations, we used the actual pH of the solution measured in each reactor and we assumed that hematite, dolomite, and calcite were solid phases present in excess (infinite phases) in the hematite, dolomite, and calcite columns, respectively. Tryptone and yeast extract were present in the growth medium but not included in the calculations because they were composed mainly of proteins, and we assumed that they did not affect the equilibriums of inorganic species. The growth medium used in the reactor filled with hematite had the highest total carbonate concentration (10 mM), and the reactors filled with dolomite and calcite had total carbonate concentrations of 4.37 and 2.97 mM, respectively. The concentration of total carbonate was adjusted in the reactor with hematite, and in the other two reactors it was established by equilibrating the solution with the mineral phase of the filling material. Table S3 in the SI shows the results of the computations.

Analytical Methods. Uranium in the influents and in the effluents from the reactors was determined using a modified procedure based on adsorptive stripping voltammetry, ASV (*18, 19*). The conditions of the measurements described in these papers could not be applied directly to our samples because our samples contained large amounts of organics; we modified and optimized the ASV for our application as described in the Supporting Information.

To determine the uranium concentrations in the biofilms, Biofilm samples of known weights were collected from the reactors and dissolved in 11 M nitric acid (J.T.Baker, cat no. 9601), then diluted with pure water and analyzed using the method described in the Supporting Information.

In the influents and effluents of the reactors, lactate concentration was determined using a lactate kit (Sigma Diagnostic, cat no. 735–10), sulfate concentration was determined using the turbidimetric method (*20*), and pH was monitored daily.

Statistical Analysis. The U(VI) immobilization rate for each reactor was calculated from the difference in U(VI) concentration between the inlet and the outlet, and the average concentrations and the standard deviations were calculated. To compare the uranium immobilization rates in the reactors, we used a two-sample *t* test (*21*). We named the average daily removal rates of the three reactors μ_{calc}, μ_{dol}, μ_{hem} for the reactors filled with calcite, dolomite, and hematite, respectively. The null hypothesis was that the average daily removal rates in the three reactors were the same ($\mu_{calc} = \mu_{dol} = \mu_{hem}$). Unpaired, two-tail tests were performed using both pooled and independent standard deviations. The calculated *t* test values ($T_{calc\text{-}dol}$, $T_{calc\text{-}hem}$, $T_{dol\text{-}hem}$) were compared with the *t* test values calculated at $t_{95,}$ showing that there was at least a 95% probability that the measured uranium removal rates were not the same, so we rejected the null hypothesis. The software DataPlot (National Institute of Standards and Technology, Gaithersburg, MD, http://www.itl.nist.gov/div898/software/dataplot.html/) was used for the calculations.

Interpretation of Microscopy Data. Procedures for sampling the biofilms for microscopy analysis and for Transmission Electron Microscopy are described in the Supporting Information. Transmission electron micrographs of cross-sectioned material showed the structure of a matured biofilm, including layers of cells, a well-developed matrix of extracellular polymers (EPS), and newly formed biominerals associated with the cells or EPS. The cells showed a heavy deposition of reduced U in their periplasmic space. Typical electron-dense precipitates coupled to the bacterial membranes contained uranium and had a poorly crystalline or nanocrystalline character, as shown by EDS and SAED.

Results and Discussions

Uranium Removal. Figure 1 shows that, as time progresses, the total amount of uranium accumulated in the biofilm increases linearly. The reactor filled with calcite was not sampled during the last 20 days because of a clogging problem experienced at that time. Note that the efficiency of uranium

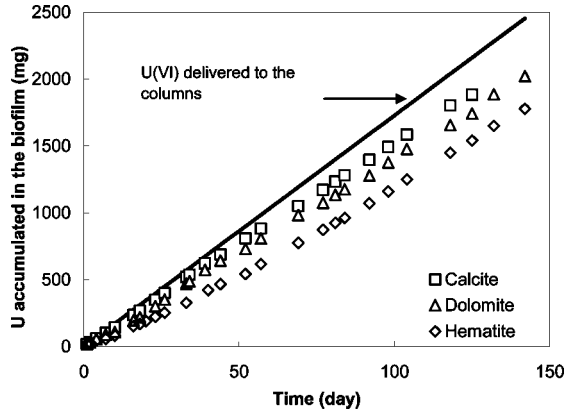

FIGURE 1. Uranium accumulated in biofilms of sulfate-reducing bacteria deposited in reactors filled with various minerals. The continuous line shows the cumulative amount of uranium delivered to each reactor (or maximum uranium accumulation possible).

TABLE 1. Average Daily Uranium Immobilization Rates in the Column Reactors

mineral on which biofilm was grown	uranium immobilization rate (mg U/day)	accumulated uranium in biofilm at the end of the experiment (mg U/g wet biofilm)
hematite	11.34 ± 2.76	4.83 ± 0.51
dolomite	14.03 ± 2.69	6.86 ± 0.58
calcite	15.31 ± 1.16	8.19 ± 0.49

removal was inversely proportional to the concentrations of carbonates in the solution: the reactor filled with hematite had the highest total carbonate concentration (10 mM), and the reactors filled with dolomite and calcite had total carbonate concentrations of 4.37 and 2.97 mM, respectively. However, since we assume that the uranium was removed enzymatically, it is not clear whether this observation is relevant. Perhaps some of the uranium was reduced by the biogenically generated hydrogen sulfide, which would explain the sensitivity of the results to the concentration of carbonates. Further analysis of this observation exceeds the boundaries of this study. The uranium immobilization efficiency evaluated at the end of the experiment was 87.2% in the reactor filled with calcite, 82.4% in the reactor filled with dolomite, and 72.5% in the reactor filled with hematite. The results demonstrate that sulfate-reducing biofilms can remove uranium from water containing carbonate in the presence of carbonate-bearing minerals. It is important for further analysis to notice that the biofilm grown in the reactor filled with hematite immobilized less uranium than the biofilms grown in the other two reactors.

Table 1 shows the average daily rates and the total amounts of accumulated uranium in each reactor. The rate of uranium immobilization in the biofilm deposited in the reactor filled with hematite is significantly lower than the rates of uranium immobilization in the biofilms deposited in the reactors filled with calcite or dolomite.

Microbial Activity and pH. Microbial activity was determined as the lactate uptake efficiency $(C_{inlet\text{-}lactate}-C_{outlet\text{-}lactate})/C_{inlet\text{-}lactate} \times 100$. The biofilms deposited in the reactors filled with hematite, dolomite, and calcite removed practically all lactate: 99.% ± 1, 98% ± 1, and 94.3% ± 0.6 of the lactate in the inlet, respectively. The average sulfate removal was 59 ± 28%, 51 ± 12%, and 24 ± 5% for hematite, dolomite, and calcite reactors, respectively. These results show that the process in the reactors was lactate limited.

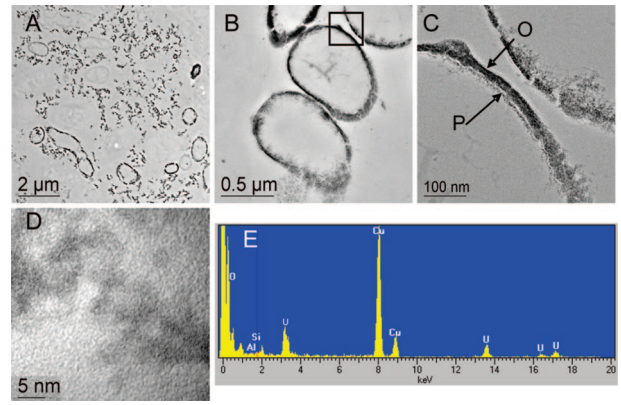

FIGURE 2. TEM images of a thin cross section of a Biofilm deposited in the reactor filled with calcite. (A) A characteristic cell population with precipitated U minerals associated with membranes and EPS. (B) Cells with reduced U(IV) in their periplasm. (C) Detail of periplasmic space with visible plasma [P] membrane and outer [O] membrane filled with U(IV) material. D) High-resolution TEM image of U-containing material reveals its poorly crystalline nanoparticulate character, with a typical particle size of 3 nm. (E) EDS spectrum showing U signal in material directly associated with cells, as well as in the dispersed material attributed to the EPS-linked particles.

The pH in the three reactors was continuously monitored during the five months of the experiment: it was 7.77 ± 0.16 in the reactor filled with hematite, 7.51 ± 0.14 in the reactor filled with dolomite, and 7.68 ± 0.14 in the reactor filled with calcite.

Characteristics of Uranium in Biofilms. *Biofilm Deposited in the Reactor Filled with Calcite.* Transmission electron micrographs (TEMs) of the Biofilm deposited in the reactor filled with calcite are shown in Figure 2A–D. Figure 2A shows that uranium deposits were associated primarily with cell membranes, as expected, but also with external polysaccharidic substances (EPS), showing as a disperse material away from the cells. Some uranium was deposited in the periplasm, (Figure 2B and C) and, as determined by EDS and SAED, the deposited material appeared to be poorly crystalline nanoparticulate (Figure 2D) with exclusive uranium and oxygen content (2E).

Biofilm Deposited in the Reactor Filled with Dolomite. TEM images of the Biofilm deposited in the reactor filled with dolomite are shown in Figure 3. Most precipitated uranium was associated with membranes and located in the periplasmic space. The preferential use of uranium as a terminal electron acceptor in periplasmic membranes, described also by Elias et al. (*22*), is evident throughout the entire sample, even though cells were frequently directly in contact with the dolomite surface (Figures 3A–D). Cells appear to have precipitated material also commonly associated with capsular structures (Figure 3E). Although no disperse EPS material like that in the calcite sample was present this time, extracellular polysaccharides certainly played a role in the accumulation of reduced material. The U-containing material appears to be nanoparticulate, very poorly crystalline, or amorphous, as shown by HRTEM and SAED (Figure 3F).

Biofilm Deposited in the Reactor Filled with Hematite. The biofilm deposited in the reactor filled with hematite showed a lower uranium removal efficiency compared to the biofilms in the reactors filled with calcite and dolomite. Its uranium deposits had a well-defined nanocrystalline structure (Figure 4), showing that the uranium deposits in the biofilm deposited in the reactor filled with hematite were more stable than

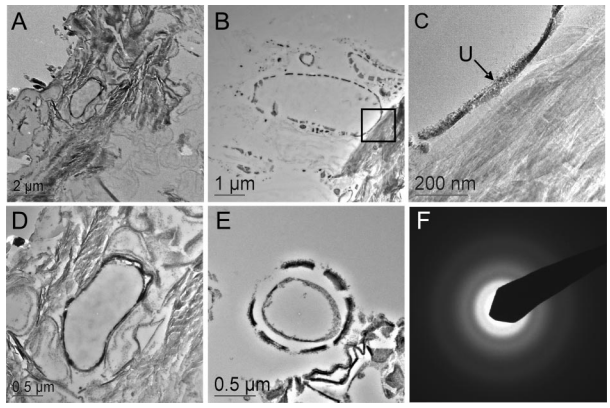

FIGURE 3. (A) TEM image of a microbial cell in close proximity to a dolomite surface shows electron-dense U(IV) precipitates. (B) Cell with heavy uranium deposits in the periplasmic space. Reduced uranium precipitated in the periplasm shown at a higher magnification (inset of B) clearly points out the more electron-dense uranium material [U] as opposed to (C) the lighter dolomite substrate. (D) Higher magnification of (A) shows membrane features and direct association with dolomite. (E) Cross section of a cell with reduced material deposited in the periplasm and (outer ring on 5E) the capsular structure. (F) SAED disperse ring pattern of the precipitated uranium demonstrates its poorly nanocrystalline or amorphous character.

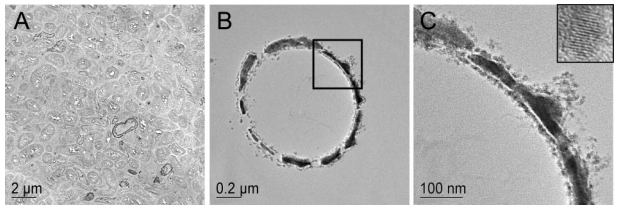

FIGURE 4. (A) TEM image of a cross section of Biofilm grown on hematite showing cells with relatively low mineral precipitation. (B) Cells that precipitated uranium demonstrated the same site of reduction-the periplasm. The square in B is shown in C. (C) Cell with pronounced lipid layer of plasma and outer membrane. HRTEM revealed the well-defined nanocrystalline character of the precipitated uranium, with a crystal size of 2–5 nm (single crystal, inset C).

those in the biofilms in the reactors filled with calcite and dolomite, which had a poorly nanocrystalline structure, Figures 2 and 3.

Precipitated Uraninite. In the reactor filled with hematite, uranium precipitated on the cell membranes and in the periplasmic spaces of the microbial cells. However, in the reactor filled with calcite, uranium also precipitated in the extracellular polymeric matrix. These observations are consistent with the reports summarized in a recent review of various studies on biologically precipitated uraninite (*23*). The crystallography of the precipitated uraninite remains controversial. It is known that uraninite occurs as crystalline particles, smaller than 3 nm, in mixed-culture incubated sediments and in pure-culture Desulfosporosinus spp. (*24*). In our study, the form of the precipitated uranium depended on the mineral phase supporting the biofilm growth: it was amorphous in the reactors filled with calcite and dolomite and crystalline in the reactor filled with hematite. The role of the mineral phase supporting biofilm growth in the crystal formation of precipitated uranium is not known, and all studies known to us, which report the crystalline structure of microbially precipitated uranite, were conducted using planktonic cultures of microorganisms, not biofilms. Our results indicate that the crystallography of uranite precipitated in biofilm reactors is affected by a factor that is not present in planktonic cultures of microorganizms, the mineral phase on which the biofilm grows.

Efficiency of Uranium Removal. Sulfate-reducing biofilms showed high removal efficiencies of uranium in the presence of carbonates: 72.5, 82.4, and 87.2% in the reactors filled with hematite, dolomite, and calcite, respectively. Previous studies showed that sulfate-reducing bacteria can reduce uranium in the presence of low concentrations of carbonates (*11, 15*) but high concentrations of carbonates inhibited uranium reduction, leading to the conclusion that uranyl–carbonate complexes are not available as electron acceptors (*25, 26*). These conclusions were reached based mostly on short-term studies and using planktonic cells only. We have demonstrated that sulfate-reducing biofilms remove uranium efficiently for long periods, under conditions resembling those expected in groundwaters in biofilms deposited on naturally occurring minerals. We therefore conclude that sulfide-reducing biofilms can be used to remove uranium from groundwaters with reasonably high efficiency, higher than 72% in our study. Table 2 summarizes our findings.

Interestingly, in the reactor filled with calcite, uranium precipitated in the matrix of extracellular polymers. We cannot explain this observation, but it is possible that uranium precipitation in the extracellular matrix was responsible for the somewhat higher overall uranium removal efficiency in that reactor. It is possible that the efficiency of uranium removal in our reactor was also affected by other factors, and not only by those we described above, such as different EPS chemistry in biofilms grown on the different minerals. The following section summarizes the known factors affecting uranium removal in microbial reactors and discusses their possible effect on our results.

Factors Controlling Uranium Removal in Microbial Reactors. *Effect of Iron.* It is well-known that Fe(III) in hematite affects the reoxidation of uranium, as formerly described (*27*), by the following reaction:

$$U(IV) + 2Fe(III) = U(VI) + 2Fe(II) \quad (1)$$

According to this reaction, the presence of ferric iron should decrease uranium reduction efficiency. Since hematite has the most Fe(III), we expect that biofilms grown on hematite should remove less uranium than biofilms grown on minerals with a smaller content of ferric iron, if this effect is indeed dominant. Biofilms grown on a hematite surface create a diffusion barrier and may prevent the access of U(VI) to solid-phase Fe(III). It is possible that the diffusion limitation created by the biofilm may be the reason why we did not observe significant differences in the rate of uranium immobilization between the biofilm grown on hematite and those grown on dolomite and calcite.

Effect of Carbonates. It is well-known that carbonates complex oxidized uranium and that these complexes are difficult to reduce. The effect of carbonates can be more subtle when the interaction between the solid-state mineral phase and uranium is considered. Zheng et al. demonstrated that calcium carbonate reduces uranium sorption on soils by forming uranyl–carbonate complexes (*28*). Our observation that the biofilms grown on calcite showed the highest removal efficiency could, hypothetically, not be explained by these interactions. However, even though the adsorption of uranium by calcite was expected to be the dominant mechanism of uranium removal in the initial stages of operation, the adsorption capacity of calcite must have been exhausted during the longer periods of time, and adsorption can not have remained the dominant mechanism of uranium removal.

Effect of Calcium. Although in natural waters the effect of calcium may be difficult to separate from the effect of carbonates, Brooks et al. claimed that uranium reduction

TABLE 2. Summary of Our Findings

mineral on which biofilm was grown	U removal efficiency (%)	iron content in mineral	extracellular uranium reduction	total carbonate (mM)	U structure	Ca^{2+} Free (mM)
hematite	72.5	Fe_2O_3 - completely iron	no	10	Well-defined nanocrystalline	2.6
dolomite	82.4	some	no	4.37	Poorly crystalline or amorphous	17.3
calcite	87.2	no	Yes (nanostructures)	2.97	Poorly crystalline	22.4

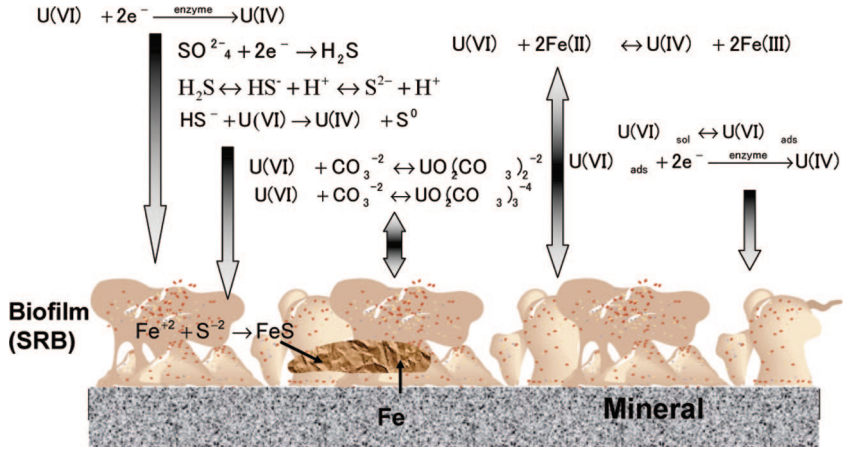

FIGURE 5. Possible mechanisms contributing to uranium precipitation/reduction/reoxidation. The figure shows biofilms grown on hematite only, however, similar mechanisms should be active in biofilms grown on calcite and dolomite.

was inhibited by the presence of calcium (*29*). In our study, the highest calcium concentration was in the reactor filled with calcite. Consequently, following the expectations based on the effect of calcium the column filled with calcite should have exhibited rather poor uranium removal. This was not the case in our study, and we offer an alternative explanation to these effects, the presence of biofilm, as described below.

Effect of Biofilm. Many studies on uranium removal have been conducted using nonbiological and well-defined systems (e.g., green rust, adsorption to hematite). As for bioremediation research, most of the experiments have been conducted in the presence of suspended microorganisms or enriched sediments (*30–32*) eventually spiked with micro and nanoparticles of other minerals (*27, 33*). Few investigations have been conducted in the presence of biofilms (*25, 34*). It is not clear which information can be transferred from one system to another, whether the results in a biofilm reactor can be explained by the observations reported in planktonic cell studies, for example. Not all our observations of uranium removal in biofilm reactors are consistent with the observations reported from studies using other systems. Therefore, we conclude that some of these inconsistencies may be related to the presence of the Biofilm and the unique environment that exists in Biofilm reactors. The conclusions based on observations of nonbiological systems may be valid for the first few days of biofilm reactor operation when the surface of the mineral is still exposed to water. As time progresses, however, less and less of the surface is exposed to bulk solution, and more and more of it is covered with the biofilm. The mass transfer resistance from the bulk to the mineral surface increases with increasing biofilm development. As a result, the chemistry near the mineral surface changes dramatically. These changes in chemistry are not uniform, though. Biofilms are heterogeneous, and their heterogeneity causes local chemistries to vary among locations (*35*). We have attempted to summarize these effects in Figure 5.

Implications of Our Study. Many authors have expressed concern about whether in situ uranium plume stabilization can be accomplished using reducing biofilms because of the presence of carbonates in groundwaters; even if bioreduction is possible, the stability of bioreduced uranium is still under discussion (*26, 36–40*). This concern is further magnified when the contaminated site contains carbonate-bearing minerals. We have demonstrated that, although the mineral type on which biofilms are grown and the total carbonate concentration affect uranium removal efficiency, over long periods of time (4–5 months) sulfate-reducing biofilms precipitate uranium and the precipitated uranium is stable as long as sulfate-reducing conditions are satisfied in the reactor. Our findings show that sulfate-reducing biofilms reduce uranium in the presence of carbonates. Since it is well-known that uranium reduction by the microbially produced sulfides is not efficient in the presence of carbonate, we conclude that the mechanism of uranium removal in the biofilm reactors was enzymatic reduction. The corollary to this conclusion is that the overall rate of the enzymatic reduction of uranium depends on the concentration of microorganisms. Consequently, the concerns raised by other authors may be justified for nonbiological systems and for planktonic cultures of microorganizms in which the concentration of microorganizms is low. In biofilms, where the concentration of microorganisms is considerably higher than it is in planktonic cultures of microorganisms, the enzymatic mechanism of uranium removal appears to be efficient enough to make a technological process of uranium immobilization possible.

Acknowledgments

We gratefully acknowledge the financial support provided by the Natural and Accelerated Bioremediation Research program (NABIR), Office of Biological and Environmental Research (OBER), U.S. Department of Energy (DOE), U.S. (grant nos. DE-FG03-01ER63270). The Pacific Northwest National Laboratory is operated for DOE by Battelle Memorial Institute under contract DE-AC06-76RL0 1830. Part of this research was performed at the Environmental Molecular Sciences Laboratory (EMSL), a national scientific user facility

sponsored by the Office of the Department of Energy, located at the Pacific Northwest National Laboratory.

Supporting Information Available

Additional details about growing biofilms and operating the column reactors, uranium determination, sampling of the biofilms for microscopy analysis, transmission electron microscopy. One figure, and three tables show additional data. This material is available free of charge via the Internet at http://pubs.acs.org.

Literature Cited

(1) U.S. EPA. Cerclis database, 49. 2007.

(2) Hua, B.; Xu, H. F.; Terry, J.; Deng, B. L. Kinetics of uranium(VI) reduction by hydrogen sulfide in anoxic aqueous systems. *Environ. Sci. Technol.* **2006**, *40* (15), 4666–71.

(3) Wersin, P.; Hochella, M. F.; Persson, P.; Redden, G.; Leckie, J. O.; Harris, D. W. Interaction between aqueous uranium(Vi) and sulfide minerals—spectroscopic evidence for sorption and reduction. *Geochim. Cosmochim. Acta* **1994**, *58* (13), 2829–43.

(4) Abdelouas, A.; Lu, Y. M.; Lutze, W.; Nuttall, H. E. Reduction of U(VI) to U(IV) by indigenous bacteria in contaminated ground water. *J. Contam. Hydrol.* **1998**, *35* (1–3), 217–33.

(5) Lovley, D. R.; Phillips, E. J. P. Reduction of uranium by *Desulfovibrio desulfuricans*. *Appl. Environ. Microbiol.* **1992**, *58* (3), 850–6.

(6) Finneran, K. T.; Anderson, R. T.; Nevin, K. P.; Lovley, D. R. Potential for Bioremediation of uranium-contaminated aquifers with microbial U(VI) reduction. *Soil Sediment Contam.* **2002**, *11* (3), 339–57.

(7) Sani, R. K.; Peyton, B. M.; Amonette, J. E.; Geesey, G. G. Reduction of uranium(VI) under sulfate-reducing conditions in the presence of Fe(III)-(hydr)oxides. *Geochim. Cosmochim. Acta* **2004**, *68* (12), 2639–48.

(8) Lovley, D. R.; Roden, E. E.; Phillips, E. J. P.; Woodward, J. C. Enzymatic iron and uranium reduction by sulfate-reducing bacteria. *Mar. Geol.* **1993**, *113* (1–2), 41–53.

(9) Francis, A. J.; Dodge, C. J.; Lu, F. L.; Halada, G. P.; Clayton, C. R. Xps and Xanes studies of uranium reduction by *Clostridium* sp. *Environ. Sci. Technol.* **1994**, *28* (4), 636–9.

(10) Behrends, T.; Van, Cappellen; P. Competition between enzymatic and abiotic reduction of uranium(VI) under iron reducing conditions. *Chem. Geol.* **2005**, *220* (3–4), 315–27.

(11) Lovley, D. R.; Phillips, E. J. P. Reduction of uranium by *Desulfovibrio desulfuricans*. *Appl. Environ. Microbiol.* **1992**, *58* (3), 850–6.

(12) Shelobolina, E. S.; Coppi, M. V.; Korenevsky, A. A.; DiDonato, L. N.; Sullivan S. A.; Konishi, H.; Xu, H.; Leang, C.; Butler, J. E.; Kim, B.-C.; Lovley, D. R. Importance of c-type cytochromes for U(VI) reduction by Geobacter sulfurreducens. *BMC Microbiol.* **2007**;*7*.

(13) Fredrickson, J. K.; Zachara, J. M.; Kennedy, D. W.; Liu, C. X.; Duff, M. C.; Hunter, D. B. Influence of Mn oxides on the reduction of uranium(VI) by the metal-reducing bacterium Shewanella putrefaciens. *Geochim. Cosmochim. Acta* **2002**, *66* (18), 3247–62.

(14) Fredrickson, J. K.; Zachara, J. M.; Kennedy, D. W.; Duff, M. C.; Gorby, Y. A.; Li, S. M. W. Reduction of U(VI) in goethite (alpha-FeOOH) suspensions by a dissimilatory metal-reducing bacterium. *Geochim. Cosmochim. Acta* **2000**, *64* (18), 3085–98.

(15) Lovley, D. R.; Phillips, E. J. P.; Gorby, Y. A.; Landa, E. R. Microbial reduction of uranium. *Nature* **1991**, *350* (6317), 413–6.

(16) Ganesh, R.; Robinson, K. G.; Chu, L. L.; Kucsmas, D; Reed, G. D. Reductive precipitation of uranium by Desulfovibrio desulfuricans: Evaluation of cocontaminant effects and selective removal. *Water Res.* **1999**, *33* (16), 3447–58.

(17) Sani, R. K.; Geesey, G.; Peyton, B. M. Assessment of lead toxicity to *Desulfovibrio desulfuricans* G20: influence of components of Lactate C medium. *Adv. Environ. Res.* **2001**, *5* (3), 269–76.

(18) Paneli, M.; Ouguenoune, H.; David, F.; Bolyos, A. Study of the reduction-mechanism and the adsorption properties of uranium(Vi)-cupferron complexes using various electrochemical techniques. *Anal. Chim. Acta* **1995**, *304* (2), 177–86.

(19) Wang, J.; Setiadji, R. Selective determination of trace uranium by stripping voltammetry following adsorptive accumulation of the uranium cupferron complex. *Anal. Chim. Acta* **1992**, *264* (2), 205–11.

(20) *Standard Methods for the Examination of Water and Wastewater*, 20th ed.; Clesceri, L. S., Eaton, A. D., Greenberg, A. E., Eds.; American Public Health Association: Washington, DC, 1998.

(21) Sdenecor, G. W., Cochran, W. G. *Statistical Methods*, 8th ed.; Iowa State University: Ames, IA, 1989.

(22) Elias, D. A.; Suflita, J. M.; McInerney, M. J.; Krumholz, L. R. Periplasmic cytochrome c(3) of *Desulfovibrio vulgaris* is directly involved in H-2-mediated metal but not sulfate reduction. *Appl. Environ. Microbiol.* **2004**, *70* (1), 413–20.

(23) Wall, J. D.; Krumholz, L. R. Uranium reduction. *Annu. Rev. Microbiol.* **2006**, *60*, 149–66.

(24) Suzuki, Y.; Kelly, S. D.; Kemner, K. M.; Banfield, J. F. Radionuclide contamination—Nanometre-size products of uranium bioreduction. *Nature* **2002**, *419* (6903), 134.

(25) Beyenal, H.; Sani, R. K.; Peyton, B. M.; Dohnalkova, A. C.; Amonette, J. E.; Lewandowski, Z. Uranium immobilization by sulfate-reducing biofilms. *Environ. Sci. Technol.* **2004**, *38* (7), 2067–74.

(26) Katsoyiannis, I. A. Carbonate effects and pH-dependence of uranium sorption onto bacteriogenic iron oxides: Kinetic and equilibrium studies. *J. Hazard. Mater.* **2007**, *139* (1), 31–7.

(27) Sani, R. K.; Peyton, B. M.; Amonette, J. E.; Geesey, G. G. Reduction of uranium(VI) under sulfate-reducing conditions in the presence of Fe(III)-(hydr)oxides. *Geochim. Cosmochim. Acta* **2004**, *68* (12), 2639–48.

(28) Zheng, Z. P.; Tokunaga, T. K.; Wan, J. M. Influence of calcium carbonate on U(VI) sorption to soils. *Environ. Sci. Technol.* **2003**, *37* (24), 5603–8.

(29) Brooks, S. C.; Fredrickson, J. K.; Carroll, S. L.; Kennedy, D. W.; Zachara, J. M.; Plymale, A. E. Inhihition of bacterial U(VI) reduction by calcium. *Environ. Sci. Technol.* **2003**, *37* (9), 1850–8.

(30) Uhrie, J. L.; Drever, J. I.; Colberg, PJS; Nesbitt, C. C. In situ immobilization of heavy metals associated with uranium leach mines by bacterial sulfate reduction. *Hydrometallurgy* **1996**, *43* (1–3), 231–9.

(31) Lovley, D. R.; Phillips, EJP. Bioremediation of uranium contamination with enzymatic uranium reduction. *Environ. Sci. Technol.* **1992**, *26* (11), 2228–34.

(32) Lovley, D. R.; Roden, E. E.; Phillips, EJP; Woodward, J. C. Enzymatic iron and uranium reduction by sulfate-reducing bacteria. *Mar. Geol.* **1993**, *113* (1–2), 41–53.

(33) Fredrickson, J. K.; Zachara, J. M.; Kennedy, D. W.; Duff, M. C.; Gorby, Y. A.; Li, S. M. W. Reduction of U(VI) in goethite (alpha-FeOOH) suspensions by a dissimilatory metal-reducing bacterium. *Geochim. Cosmochim. Acta* **2000**, *64* (18), 3085–98.

(34) Marsili, E.; Beyenal, H.; Di Palma, L.; Merli, C.; Dohnalkova, A.; Amonette, J. E. Uranium removal by sulfate reducing biofilms in the presence of carbonates. *Water Sci. Technol.* **2005**, *52* (7), 49–55.

(35) Beyenal, H.; Lewandowski, Z. Dynamics of lead immobilization in sulfate reducing biofilms. *Water Res.* **2004**, *38* (11), 2726–36.

(36) Kelly, S. D.; Kemner, K. M.; Brooks, S. C. X-ray absorption spectroscopy identifies calcium-uranyl-carbonate complexes at environmental concentrations. *Geochim. Cosmochim. Acta* **2007**, *71* (4), 821–34.

(37) Luo, J.; Weber, F.-A.; Cirpka, O. A.; Wu, W.-M.; Nyman, J. L.; Carley, J., Jardine, P. M.; Criddle, C. S.; Kitanidis, P. K. Modeling in-situ uranium(VI) bioreduction by sulfate-reducing bacteria. *J. Contam. Hydrol.* **2007**.

(38) Lloyd, J. R.; Renshaw, J. C. Bioremediation of radioactive waste: radionuclide-microbe interactions in laboratory and field-scale studies. *Curr. Opin. Biotechnol.* **2005**, *16* (3), 254–60.

(39) Wan, J. M.; Tokunaga, T. K.; Brodie, E; Wang, Z. M.; Zheng, Z. P.; Herman, D. Reoxidation of bioreduced uranium under reducing conditions. *Environ. Sci. Technol.* **2005**, *39* (16), 6162–9.

(40) Gu, B. H.; Wu, W. M.; Ginder-Vogel, M. A.; Yan, H; Fields, M. W.; Zhou, J. Bioreduction of uranium in a contaminated soil column. *Environ. Sci. Technol.* **2005**, *39* (13), 4841–7.

ES071335K